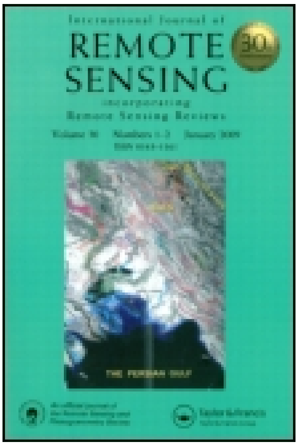

International Journal of Remote Sensing
Publication details, including instructions for authors and subscription information:
http://www.tandfonline.com/loi/tres20

Role of sea-surface wind and transport on enhanced aerosol optical depth observed over the Arabian Sea

P. Sivaprasad [a] & C. A. Babu [a]

[a] Department of Atmospheric Sciences, Cochin University of Science and Technology, Cochin, 682 022, India

To cite this article: P. Sivaprasad & C. A. Babu (2012): Role of sea-surface wind and transport on enhanced aerosol optical depth observed over the Arabian Sea, International Journal of Remote Sensing, 33:16, 5105-5118

To link to this article: http://dx.doi.org/10.1080/01431161.2012.657373

International Journal of Remote Sensing
Vol. 33, No. 16, 20 August 2012, 5105–5118

Role of sea-surface wind and transport on enhanced aerosol optical depth observed over the Arabian Sea

P. SIVAPRASAD* and C. A. BABU
Department of Atmospheric Sciences, Cochin University of Science and Technology, Cochin 682 022, India

(*Received 29 September 2010; in final form 23 November 2011*)

The objective of this study is to understand the reasons for the enhancement in aerosol optical depth (AOD) over the Arabian Sea observed during June, July and August. During these months, high values of AOD are found over the sea beyond 10° N and adjacent regions. The Arabian Sea is bounded by the lands of Asia and Africa on its three sides. So the region is influenced by transported aerosols from the surroundings as well as aerosols of local origin (marine aerosols). During the summer monsoon season in India, strong surface winds with velocities around 15 m s^{-1} are experienced over most parts of the Arabian Sea. These winds are capable of increasing sea spray activity, thereby enhancing the production of marine aerosols. The strong winds increase the contribution of marine aerosols over the region to about 60% of the total aerosol content. The main components of marine aerosols include sea salt and sulphate particles. The remaining part of the aerosol particles comes from the western and northern land masses around the sea, of which the main component is transported dust particles. This transport is observed at higher altitudes starting from 600 m. At low levels, the transport occurs mainly from the Indian Ocean and the Arabian Sea itself, indicating the predominance of marine aerosols at these levels. The major portion of the total aerosol loading was contributed by coarse-mode particles during the period of study. But in the winter season, the concentration of coarse-mode aerosols is found to be less. From the analysis, it is concluded that the increase in marine aerosols and dust particles transported from nearby deserts results in an increase in aerosol content over the Arabian Sea during June, July and August.

1. Introduction

Aerosols are classified into natural and anthropogenic, according to their origin. Sea salt, dust, natural sulphates, etc., are naturally occurring aerosols, whereas soot, industrial sulphates, black carbon, etc., are of anthropogenic origin. Soot is an absorbing aerosol whereas dust and organic matter are partly absorbing. Sea salt and sulphates mostly reflect radiation. So the insertion of different types of aerosols significantly changes the radiation budget of the Earth's atmospheric system. Global warming produced by greenhouse gases is partly suppressed by aerosols; they therefore have a substantial role in the radiation budget and climate (Charlson *et al*. 1992, IPCC 1995). The radiative effects of aerosols on the Earth's atmospheric system are governed by

---

*Corresponding author. Email: sivaatm@gmail.com

International Journal of Remote Sensing
ISSN 0143-1161 print/ISSN 1366-5901 online
http://www.tandf.co.uk/journals
http://dx.doi.org/10.1080/01431161.2012.657373

the quantity of aerosols in the atmosphere, their vertical distribution, size distribution and single scattering albedo, and the reflectivity of the underlying surface (Pilnis *et al*. 1995).

One of the largest uncertainties in climate change studies comes from the climate forcing caused by tropospheric aerosols (Hansen *et al*. 1997). So monitoring aerosols on regional and global scales is crucial for understanding changes in radiation flux. Nowadays, ground-based and satellite sensors are available for continuous monitoring of aerosols. Of these, satellite remote sensing is one of the promising tools that provide aerosol distributions on regional and global scales (Ferrare *et al*. 1990, Kaufman *et al*. 1997). However, the assessment of Moderate Resolution Imaging Spectroradiometer (MODIS)-derived aerosol optical depth (AOD) relative to the Aerosol Robotic Network (AERONET) suggests that small uncertainties in calibration can lead to spurious conclusions about the trend of long-term aerosol property distribution (Levy *et al*. 2010). Radiative transfer models along with satellite-derived data can provide information about the radiative effects of individual aerosol plumes (Christopher *et al*. 1996).

In the present study, the possible reasons for enhancement in AOD over the Arabian Sea during June, July and August are examined. The Arabian Sea is located in the northwest Indian Ocean. It is bounded by India (to the east), Pakistan and Iran (to the north), and the Arabian Peninsula (in the west). The Gulf of Oman is located in the northwest corner of the Arabian Sea. During the summer monsoon season, the region is affected by strong southwesterly winds. The Somali jet appears over the sea during the summer season of the northern hemisphere. The wind direction over the Arabian Sea is southwesterly (towards the northeast) during the southwest monsoon season (June–September) and northeasterly (towards the southwest) during the northeast monsoon season (October and November). During the other months, feeble winds are observed over the region.

Many studies on aerosols have been performed over the Arabian Sea and its adjoining regions. The study by Vinoj and Satheesh (2003) reveals that wind has a significant role in AOD and radiative forcing over the Arabian Sea during the summer monsoon months of July and August. The variability observed in wind magnitude and direction during normal and drought years plays an important role in the variability of AOD observed over the Arabian Sea during the mid-monsoon month of July (Rahul *et al*. 2008). The study by Babu *et al*. (2008) also infers the impact of seasonal changes in wind pattern on aerosol characteristics and their effect on forcing efficiency over the sea. Susan and Prabha (2008) showed that during the pre-monsoon months, high-mass concentrations of aerosols are observed over the northern and eastern parts (west coast of India), and non-sea-salt aerosols dominate to about 76% of the total aerosol mass during the season. The analysis by Kalappureddy *et al*. (2009) indicates that the dominant aerosol types change significantly in the coastal, middle and far regions of the Arabian Sea during the pre-monsoon season. Using the collection 5 MODIS data, Remer *et al*. (2008) showed that the global mean AOD over oceans at the 550 nm wavelength is 0.13 and that under high-AOD conditions, fine-mode aerosols dominate over relatively large dust particles over all oceans except the tropical Atlantic downwind of the Sahara and during some months over the Arabian Sea. The deserts surrounding the sea are prominent sources of natural dust aerosols. These deserts include the Thar Desert in India and Pakistan and the Arabian and Nubian deserts of Africa. Since the sea is surrounded by these land masses, the possibility of transport of continental aerosols towards the sea is greater Transport of continental aerosols towards the Arabian Sea and the Bay of Bengal from the Indian subcontinent, Arabia and southeast Asia during January–March is reported by Rajeev *et al.* (2000). Advection of continental air masses towards the sea brings both natural and anthropogenic aerosols into the atmosphere. Satheesh and Srinivasan (2002) demonstrated that over the southern Arabian Sea, during April/May, there exists significant transport of dust aerosols from the Saharan/Arabian regions, when northwesterly winds prevail. Besides the transported particles, the main source of aerosols over the oceanic regions is the sea-salt aerosols originating from the wave-breaking activity of sea-surface wind. The production of sea-salt aerosols depends on the strength of the surface wind. A recent study by Korhonen *et al.* (2010) reveals that the increase in sea spray flux caused by an increase in wind speed resulted in an increment in AOD over the southern hemisphere.

Sea-salt aerosols scatter solar radiation and the forcing caused by these aerosols causes a cooling effect globally (Dobbie *et al.* 2003). The change in the chemical composition of aerosols with changes in sea-surface wind alters the radiative properties of the atmosphere, and this has to be taken into account in algorithms used for retrieval of aerosol and sea-surface temperature from satellite data (Satheesh 2002). The presence of mineral dust over land and oceans causes surface cooling (by scattering and absorption) and lower atmospheric heating (by absorption). Then, low-level inversion is intensified and thereby convection is reduced (Satheesh and Moorthy 2005). Anthropogenic aerosols also play a significant role in the radiation balance of the Earth's atmospheric system. Therefore the sources and transportation of these aerosols in the atmosphere are essential factors to be included in climate studies.

2. Data and methodology

The 558 nm data from the level-3 Multi-angle Imaging Spectroradiometer (MISR) onboard the Terra satellite were used for analysing the spatial and temporal variation of AOD. The resolution of the data set is $0.5^\circ \times 0.5^\circ$. MISR observes the Earth globally at nine different angles, ranging from 70° forward to 70° backward, and gives information at four spectral bands (446, 558, 673 and 866 nm) (Diner *et al.* 2002). High sensitivity is provided by the instrument due to its oblique viewing, with optical depth values showing good agreement with the data derived from AERONET ground-based observations (Abdou *et al.* 2005, Kahn *et al.* 2005). The studies show a high correlation between MISR- and AERONET-observed AODs over oceanic regions and less correlation over desert regions. Here we used the data at a visible wavelength. Variation in the aerosol parameters, such as AOD, Ångström exponent and mass concentration, for different months are studied for the period from 2001 to 2009. The Ångström exponent is derived from the AOD values obtained at 558 and 866 nm wavelengths using the following formula,

$$\alpha = -\frac{\log_{10}(\tau_{\lambda 1}/\tau_{\lambda 2})}{\log_{10}(\lambda 1/\lambda 2)}, \qquad (1)$$

where α is the Ångström exponent and τ_λ is the AOD measured at wavelength λ. The Ångström exponent is inversely related to the average size of particles, so it is useful for assessing the average particle size of atmospheric aerosols: the smaller the particle, the larger the exponent.

The wind pattern over the region is analysed using National Centers for Environmental Prediction/National Center for Atmospheric Research (NCEP/NCAR) re-analysis wind data (Kalnay *et al*. 1996) with 2.5° × 2.5° resolution. The data are available in 17 pressure levels of which 925 hPa wind is used in the present study to understand the surface wind pattern. Monthly Global Precipitation Climatology Project (GPCP) rainfall (1° × 1°) data (Adler *et al*. 2003) are used for obtaining the rainfall pattern over the study area. Here, data from about 6000 rain gauges, geostationary and low-orbit satellites and passive microwave and sounding observations are merged to obtain monthly estimates of globally gridded rainfall from 1979. From the rainfall distribution, we identify the situation for wet removal of aerosol particles. The Environmental Satellite (Envisat)/SCIAMACHY absorbing aerosol index (AAI) (1° × 1.25° resolution) is used in order to understand the presence of dust aerosols over the Arabian Sea region. The mission objectives and measurement modes of SCIAMACHY are described by Bovensmann *et al*. (1999). The ultraviolet absorbing index obtained from level-3 Aura/OMI (ozone measuring instrument) is also analysed for confirmation of the results obtained using the SCIAMACHY instrument. The resolution of these data is 1° × 1°. A detailed description of the sensor is given by Levelt *et al*. (2006). AAI is measured in the ultraviolet region of the spectrum and it indicates the presence of absorbing aerosols, such as dust and black carbon.

3. Results and discussion

3.1 *Spatial distribution of aerosols over the Arabian Sea and adjoining areas*

From a general pattern obtained from MISR data (figure 1), it is observed that during July, AOD increases to high values over the Arabian Sea and adjoining areas to the north and west coasts of the sea. To the west of the sea, the Arabian Desert shows a high concentration of aerosols with optical depth values above 0.6. AOD is found to be high over the northern parts, including Pakistan and some parts of the Indian subcontinent. The distribution pattern is found to be almost the same for June and August. This shows that some mechanisms contribute towards the high loading of aerosols over the Arabian Sea during the June–August period. Over the Indian subcontinent, data are missing in some parts due to the presence of monsoon clouds. Thick clouds obstruct the passage of radiation, which results in a loss of data over these regions. Less aerosol loading is expected in India since the months fall within the summer monsoon season and intense rainfall activity occurs over the region. High AOD is seen over the north-west areas of the country, where the Thar Desert is located.

In the present study we are interested in the distribution of aerosols over the Arabian Sea. AOD values are found to be 0.8–1.2 over most parts of the sea beyond 10° N during June–August. The region with rich aerosol content extends up to 30° N. This is a peculiar feature since pristine air masses are expected over the oceanic region. Moving to the south of 10° N, a gradual decrease in AOD can be seen with the smallest value below 0.2 to the south of 5° N. Over a few parts of the Bay of Bengal also, high AOD is observed, but it is confined to small pockets, different from that detected over the Arabian Sea. During other months, high AOD of about 0.6–0.8 is observed over the northern parts of India, especially in the Indo-Gangetic plain. All of south India, the Bay of Bengal and the Arabian Sea show less aerosol loading. Values around 0.2 over almost the entire Arabian Sea indicate less aerosol loading over the sea and the southern parts of India during the remaining months. Over the Arabian Desert, AOD is found to be high during April and July, with values around 0.7. During the other

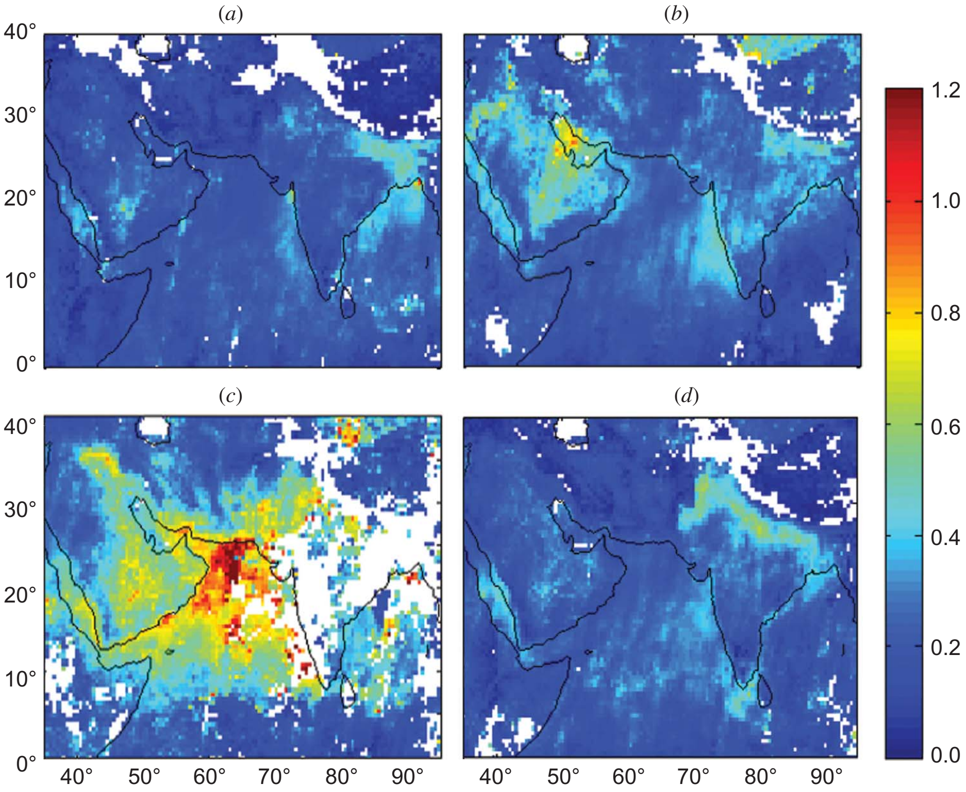

Figure 1. Terra MISR AOD for (*a*) January, (*b*) April, (*c*) July and (*d*) November 2007.

months, the desert is calm and the optical depth remains below 0.4. This indicates relatively high production of dust aerosols over the desert during the summer season, in comparison with that for the boreal winter season.

3.2 *Monthly variation of aerosol parameters over the Arabian Sea*

The monthly variations in AOD and the Ångström exponent averaged for 2001–2009, with their spread, for a region bounded by 19° N–24° N and 60° E–65° E over the Arabian Sea, obtained from MISR observations are shown in figures 2 and 3. The region belongs to the north Arabian Sea and is characterized by high aerosol loading during the period of study. MISR data at 558 nm (green band) are used to analyse the AOD pattern. The wavelength is in the visible region of the spectrum (the largest percentage of incoming solar radiation consists of visible wavelengths) and interacts mainly with the accumulation-mode aerosols. High AOD in the range 0.7–1.0 is observed in June, July and August for almost all years. During the remaining months, the AOD values range from 0.2 to 0.5, with minimum values in the winter months from November to February. The analysis indicates a lower aerosol concentration over the Arabian Sea from September to May. The highest aerosol concentration is detected in July. The mean optical depth is observed to be around 1.0 during the month. Thus during June, July and August, the AOD values shoot up even in the marine environment.

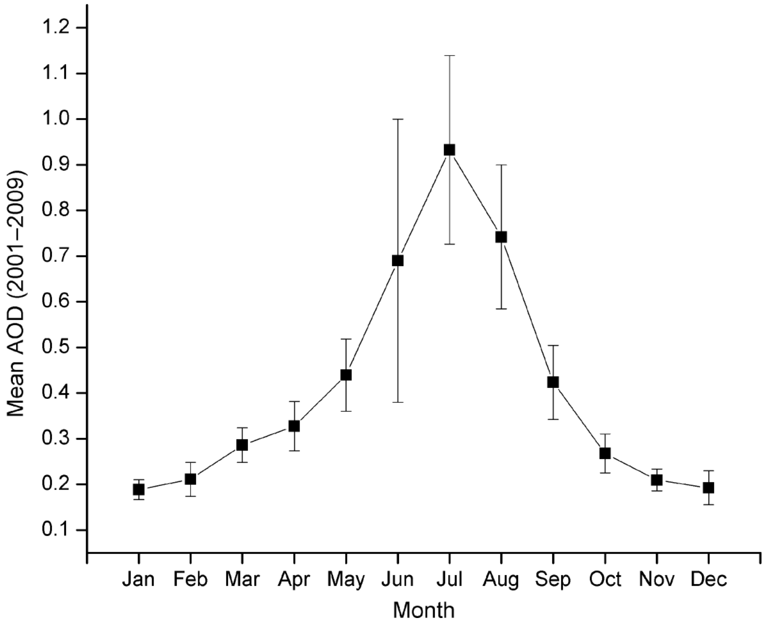

Figure 2. Monthly variation of AOD over the region (19° N–24° N and 60° E–65° E) averaged for 2001–2009.

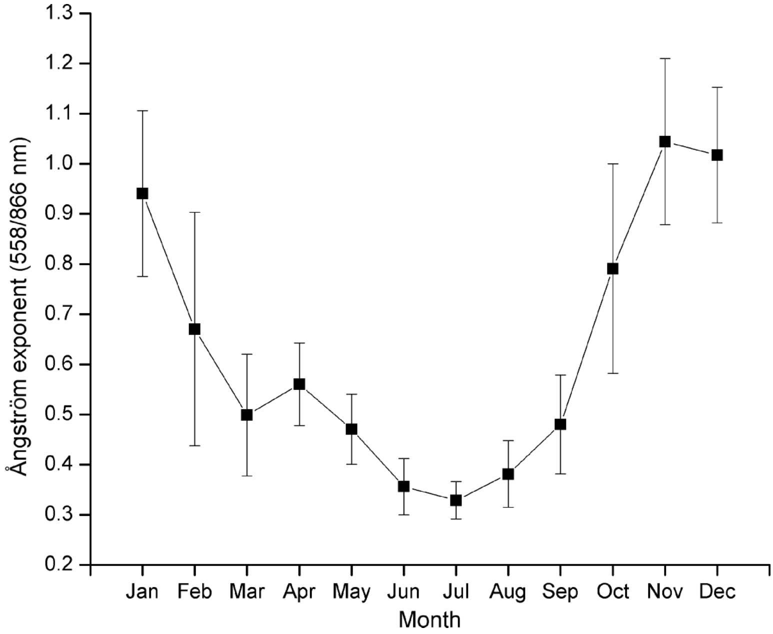

Figure 3. Monthly variation of the Ångström exponent over the region (19° N–24° N and 60° E–65° E) averaged for 2001–2009.

The Ångström exponent, which indicates the average size of the aerosol particles in the atmosphere, decreases from March and continues to be low up to September. The maximum Ångström exponent, around 1.0, is observed during the period November–January. The exponent is at a minimum, with values around 0.4, during June, July and August, and moderate values are detected in the remaining months. These factors obviously show that coarse-mode aerosols are prominent during the period of study (June–August). It is clear from the figure that during summer months, relatively large aerosol particles contribute to a major fraction of the total aerosol content. On the other hand, the high Ångström exponent in the northern hemisphere winter season is an indication of a relatively high concentration of accumulation-mode aerosols, i.e. aerosols of smaller size. This agrees with the study by Chauhan *et al*. (2009), which showed a high Ångström exponent over the sea during the winter month of December, indicating the presence of smaller particles, which are advected from the Indian subcontinent. The accumulation-mode aerosols are assumed to be originating mainly from anthropogenic activities. Sea salt is included in the coarse-mode aerosols and an increase in these particles can affect the Ångström exponent significantly.

3.3 *Enhancement of AOD by sea-surface wind*

The role of sea-surface winds on AOD is analysed using NCEP/NCAR monthly U (zonal component) and V (meridional component) wind data. The surface wind pattern averaged for June, July and August is shown in figure 4. Except in the eastern parts of the Arabian Sea, the wind speed is nearly 15 m s^{-1}. The speed is around 10 m s^{-1} in the eastern parts of the sea. In the south-east region, less than 10 m s^{-1} wind is observed. Over the Bay of Bengal, wind speed of around 10 m s^{-1} is observed. The wind observed over the region is part of the low-level jet (LLJ) associated with the summer monsoon season in India. The maximum wind core of the LLJ is at an altitude of around 1.5 km (850 hPa), and the wind has its maximum strength in the

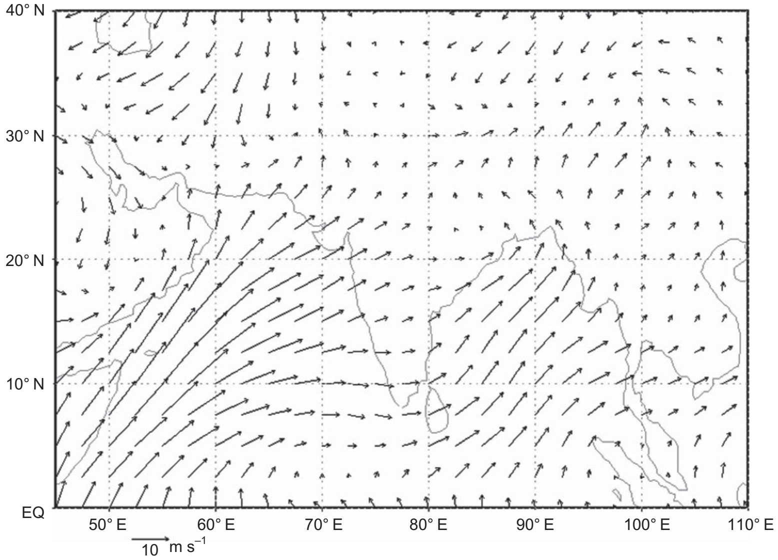

Figure 4. Average surface wind (m s^{-1}) for June, July and August 2007.

Arabian Sea and on the west coast of India. The core of the wind is found to have a strength of 20–25 m s^{-1}. During other months, the winds are feeble and are aligned in a random manner. Over the tropical Indian Ocean, the AOD is related to the wind speed according to the equation

$$\tau_a = \tau_o \exp(bU), \tag{2}$$

where τ_o is the AOD at 0 wind speed and b is a constant whose value is 0.12 for 500 nm, 0.17 for 850 nm and 0.18 for 1020 nm (Satheesh 2002). U is the observed wind speed. By using the least square method, the value of b is obtained as 0.12202 for a 550 nm wavelength. So, we have used the value 0.12 for computation of the contribution of marine aerosols due to monsoon winds. Substituting the wind speed of 15 m s^{-1} in the above equation, a τ_a value of 0.72 is obtained. This is much higher compared with the aerosol concentration obtained during the other months over the sea and amounts to about 60% of the total AOD. Thus, the enhanced marine aerosols due to the strong sea-surface wind contribute more than half of the total aerosol loading during June, July and August.

Sea salt is hygroscopic in nature and can be removed from the atmosphere by washout or wet removal. Washout occurs due to the formation of cloud droplets by the condensation of water vapour over the particles. Wet removal happens due to raindrops, which diffuse aerosols in their path towards the Earth's surface. The monthly rainfall pattern over the region is analysed to understand the washout or wet removal. The rainfall pattern for July is shown in figure 5. Most parts of the Indian subcontinent, the eastern parts of the Arabian Sea and the Bay of Bengal receive rainfall of more than 150 mm. But over the other parts of the Arabian Sea, rainfall is less than 30 mm. The chance of wet removal is less in comparison with the Indian mainland. So the particles can remain in the atmosphere for a comparatively long period. This also favours a high aerosol concentration over the Arabian Sea.

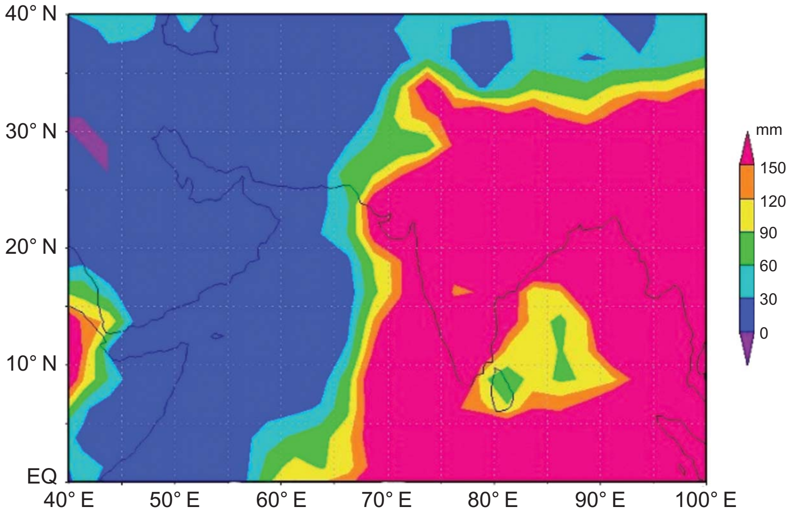

Figure 5. GPCP rainfall (mm) for July 2007.

3.4 *Role of transport from the surroundings*

Transport of aerosols towards the study area is shown in figure 6 using the hybrid single particle Lagrangian integrated trajectory (HYSPLIT) model. The inputs to the model are the NCEP/NCAR 17 pressure-level re-analysis wind data, re-processed into the HYSPLIT-compatible format available on the Air Resources Laboratory's (ARL's) website. Here, a particle model is used, in which a fixed number of initial particles are advected about the model domain by the mean wind field and a turbulent component. The advection of a particle or puff is computed from the average of the three-dimensional velocity vectors for the initial position at time t, $P(t)$, and the first-guess position at time $t + \Delta t$, $P'(t + \Delta t)$.

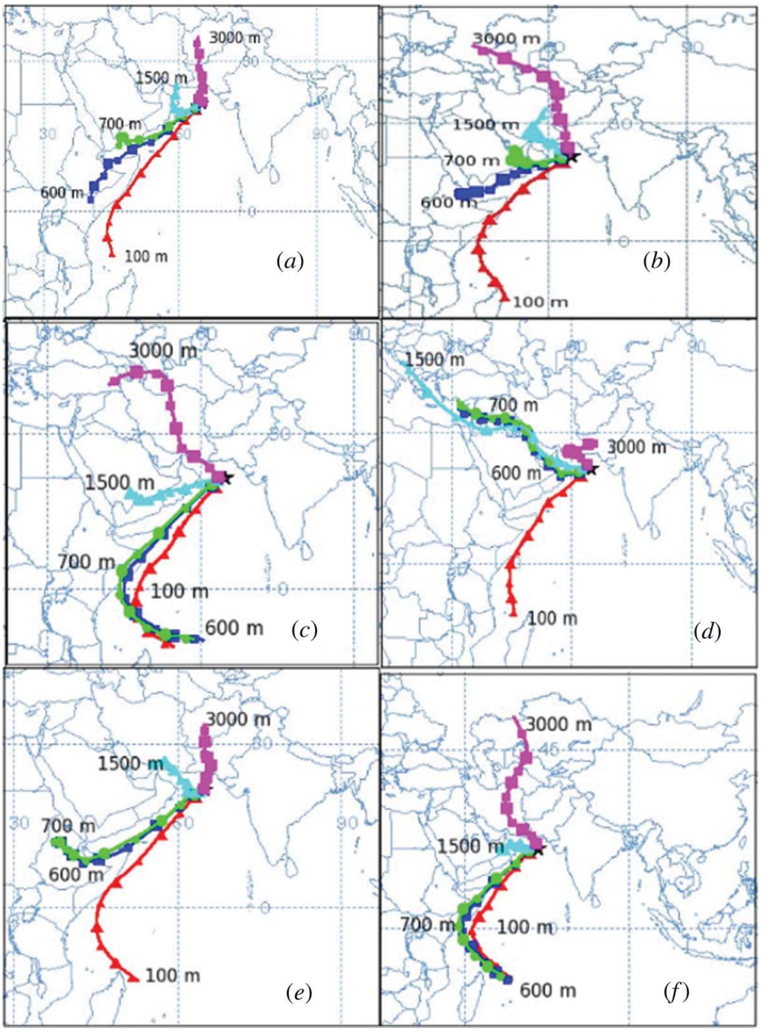

Figure 6. NOAA HYSPLIT back trajectory analysis for (*a*) 15 June 2007, (*b*) 15 July 2007, (*c*) 15 August 2007, (*d*) 15 June 2008, (*e*) 15 July 2008 and (*f*) 15 August 2008 at 100, 600, 700, 1500 and 3000 m altitudes.

We made a number of analyses by running the model for five days backward during June–August of 2001–2009 to understand the advection of air masses and transport of particles towards the area of interest. A few representative cases are shown in figure 6. It is found that during the study period, at low levels, the back trajectory is confined to the area over the oceanic region, including the Indian Ocean and the Arabian Sea itself. On the way towards the Arabian Sea, it touches the Somalian coast. Going to high altitude, the trajectory covers Ethiopia, Yemen and Oman. Above 1500 m altitude, the air mass comes from land areas lying to the west and north parts of the sea (Arabian Desert, Gulf of Oman, Afghanistan and Pakistan). The pattern is almost similar for June–August. Thus, in general, during the months of study, the transport of aerosols towards the sea occurs from the Indian Ocean, and the north and west coasts mentioned above. The mineral dust sources around the northern Indian Ocean were identified by Leon and Legrand (2003). They found that the main dust sources are located in the Nubian Desert, the Arabian Peninsula, Iran, Pakistan, Afghanistan, northwest India and Somalia. The frequency of dust events is maximal in the spring and summer months for most of the above areas.

The intense LLJ associated with the southwest monsoon over India can provide a pathway for the dust particles from the Horn of Africa, particularly from the deserts in Somalia, towards the central Arabian Sea (Clemens *et al*. 1991). Going to higher levels, the dust particles from the Arabian Desert, Pakistan and Afghanistan are transported towards the Arabian Sea. This is an indication of the presence of continental aerosols over the region besides marine aerosols. The predominant component in transported aerosols is the mineral dust particles originating from the land masses mentioned above.

The Envisat/SCIAMACHY AAI is used to confirm the presence of dust aerosols (figure 7). The instrument derives the AAI from the reflectance intensity

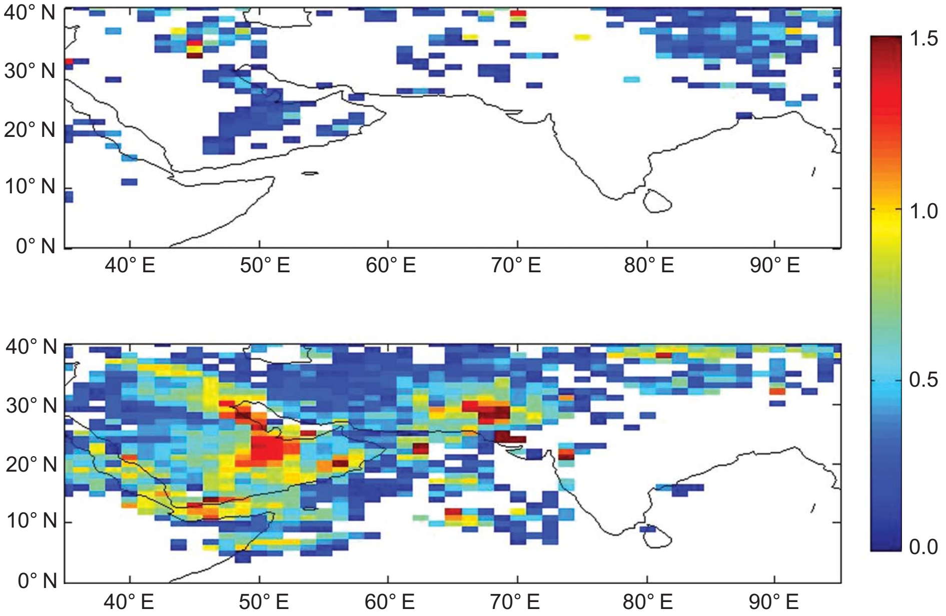

Figure 7. Envisat/SCIAMACHY AAI for (*a*) January and (*b*) July 2007.

measurements at 380 and 340 nm wavelengths. In the ultraviolet region of the spectrum, dust and black carbon are absorbing in nature. A positive value of AAI indicates the presence of these aerosols. Although the instrument is mainly used to detect industrial and biomass burning aerosols, in the absence of such aerosols, the main contributors, which absorb the ultraviolet light, are dust particles. We do not expect a high concentration of black carbon aerosols over the desert regions. So the positive AAI detected over the desert regions is considered to originate from dust aerosols. January and July are presented in the figure. Only positive values of AAI are included here. The white colour indicates missing data or negative AAIs, which represent the scattering aerosols. Over the Arabian Sea, during July, positive AAI can be observed. A higher value around 1.5 is found over the northern, central and western coasts of the sea. The land areas in the northern and western parts of the sea show high AAI during the month. So the possibility of transport of dust aerosols from these locations can be justified. Some parts of northwest India also have intense dust aerosol concentration. The same pattern can be observed for June and August. During January we cannot find positive AAI over the entire Arabian Sea. Over the land areas around the sea, AAI is less in comparison with the summer months. This is due to lack of turbulence during winter months.

The Aura/OMI ultraviolet aerosol index is also analysed for the same months over the same location. The results are shown in figure 8. OMI data also provide similar information on aerosols to that obtained from Envisat/SCIAMACHY. OMI shows the same pattern of aerosol distribution over the sea and its adjoining areas. The ultraviolet aerosol index is found to be above 1.5 over the northern and western parts of the sea. It is around 1.2 over the central Arabian Sea and relatively fewer values are observed over the east coast. Over the Arabian Desert, a high aerosol index above 2.0 is observed. To the north of the sea, also, the aerosol index is found to be high.

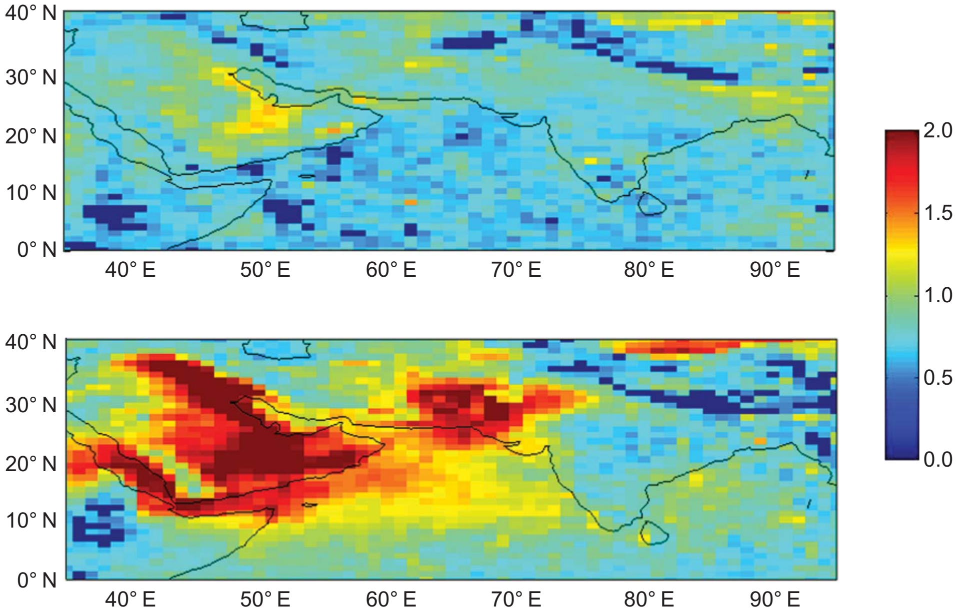

Figure 8. OMI ultraviolet aerosol index for (*a*) January and (*b*) July 2007.

These regions include Pakistan and a few parts of India. This clearly supports the transport of aerosols from the western and northern lands towards the Arabian Sea. However, during the other months, the aerosol index is less over the sea. From the figure it is obvious that in January the index is less, with values of around 0.5 over most parts of the Arabian Sea and its nearby areas. A relatively high value is observed over a small area in the Arabian Desert. These results strengthen the findings from the SCIAMACHY instrument. In other words, we infer the presence of dust particles over the Arabian Sea during the period of study.

4. Conclusions

During June, July and August, the aerosol concentration increases over the Arabian Sea and its surrounding land masses. Aerosol loading is high throughout the year over the northern parts of India, especially over the Gangetic plain. On the other hand, lower AOD values are observed most of the time in the southern parts of the subcontinent. AOD is found to be high over the Arabian Desert during the boreal summer months. Strong monsoon winds are observed over the Arabian Sea during the period of study. The contribution of marine aerosols is high (exceeding more than half of the total aerosol content) due to the turbulence and sea spray activity over the sea surface produced by the strong winds. The other prominent aerosol component is the dust particles transported from the western and northern land masses around the sea. From the weak rainfall activity observed over the region, we can conclude that the chance of wet removal is less. Thus the enhancement in marine aerosols and transported dust particles is responsible for the high aerosol loading observed over the Arabian Sea during June, July and August.

Acknowledgements

The authors acknowledge GIOVANNI for providing analysis and visualization tools and NOAA for the HYSPLIT model. The first author is grateful to UGC for providing a research fellowship.

References

Abdou, W.A., Diner, D.J., Martonchik, J.V., Bruegg, C.J., Kahn, R.A., Gaitley, B.J., Crean, K.A., Remer, L.A. and Holben, B., 2005, Comparison of coincident multiangle imaging spectroradiometer and moderate resolution imaging spectroradiometer aerosol optical depths over land and ocean scenes containing aerosol robotic network sites. *Journal of Geophysical Research*, **110**, D10S07, doi:10.1029/2004JD004693.

Adler, R.F., Huffman, G.J., Chang, A., Ferraro, R., Xie, P., Janowik, J., Rudolf, B., Schueider, U., Curtis, S., Bolvin, D., Gruber, A., Susskind, J., Arkin, P. and Nelkin, E., 2003, The version-2 Global Precipitation Climatology Project (GPCP) monthly precipitation analysis (1979–present). *Journal of Hydrometeorology*, **4**, pp. 1147–1167.

Babu, S.S., Nair, V.S. and Moorthy, K.K., 2008, Seasonal changes in aerosol characteristics over Arabian Sea and their consequence on aerosol short-wave radiative forcing: results from ARMEX field campaign. *Journal of Atmospheric and Solar-Terrestrial Physics*, **70**, pp. 820–834.

Bovensmann, H., Burrows, J.P., Buchwitz, M., Frerick, J., Noel, S. and Rozanov, V.V., 1999, SCIAMACHY: mission objectives and measurement modes. *Journal of Atmospheric Sciences*, **56**, pp. 127–150.

Charlson, R.J., Schewartz, S.E., Hales, J.M., Cess, R.D., Coakley, J.A., Hansen, J.E. and Hofmann, D.J., 1992, Climate forcing by anthropogenic aerosols. *Science*, **255**, pp. 423–430.

Chauhan, P., Sanwlani, N. and Navalgund, R.R., 2009, Aerosol optical depth variability in the northeastern Arabian Sea during winter monsoon: a study using in-situ and satellite measurements. *Indian Journal of Marine Sciences*, **38**, pp. 390–396.

Christopher, S.A., Kliche, D.V., Chou, J. and Welch, R.M., 1996, First estimates of the radiative forcing of aerosols generated from biomass burning using satellite data. *Journal of Geophysical Research*, **101**, pp. 21265–21273.

Clemens, S., Prell, W., Murray, D., Shimmield, G. and Weedon, G., 1991, Forcing mechanisms of the Indian Ocean monsoon. *Nature*, **353**, pp. 720–725.

Diner, D.J., Beckert, J.C., Hothwell, G.W. and Rodriguez, J.I., 2002, Performance of the MISR instrument during its first 20 months in Earth orbit. *IEEE Transactions on Geoscience and Remote Sensing*, **40**, pp. 1449–1466.

Dobbie, S., Li, J., Harvey, R. and Chylek, P., 2003, Sea-salt optical properties and GCM forcing at solar wavelengths. *Atmospheric Research*, **65**, pp. 211–233.

Ferrare, R.A., Fraser, R.S. and Kaufman, Y.J., 1990, Satellite measurements of large-scale air pollution: measurements of forest fire smoke. *Journal of Geophysical Research*, **95**, pp. 9911–9925.

Hansen, J., Sato, M. and Ruedy, R., 1997, Radiative forcing and climate response. *Journal of Geophysical Research*, **102**, pp. 6831–6864.

Intergovernmental Panel on Climate Change (IPCC) Scientific Assessment Group, 1995, Radiative forcing of climate change. In *Climate Change 1994: Radiative Forcing of Climate Change and an Evaluation of the IPCC 1992 IS92 Emission Scenarios*, J.T. Houghton, L.G. Meira Filho, J. Bruce, H. Lee, B.A. Callander, E. Haites, N. Harris and K. Maskell (Eds.) (New York: Cambridge University Press).

Kahn, R.A., Gaitley, B., Martonchik, J., Diner, D.J., Crean, K.A. and Holbon, B., 2005, Multiangle Imaging Spectroradiometer (MISR) global aerosol optical depth validation based on 2 years of coincident Aerosol Robotic Network (AERONET) observations. *Journal of Geophysical Research*, **110**, D10S04, doi:10.1029/2004JD004706.

Kalappureddy, M.C.R., Kaskaoutis, D.G., Raj, P.E., Devara, P.C.S., Kambezidis, H.D., Kosmopoulos, P.G. and Nastos, P.T., 2009, Identification of aerosol type over the Arabian Sea in the premonsoon season during the Integrated Campaign for Aerosols, Gases and Radiation Budget (ICARB). *Journal of Geophysical Research*, **114**, D17203, doi:10.1029/2009JD011826.

Kalnay, E., Kanamitsu, M., Kistler, R., Collins, W., Deaven, D., Gandin, L., Iredell, M., Saha, S., White, G., Woollen, J., Zhu, Y., Chelliah, M., Higgins, W., Janowim, J., Mo, K.C., Roopelewski, C., Wang, J., Leetmaa, A., Reynolds, R., Jenne, R. and Joseph, D., 1996, The NCEP/NCAR 40 year reanalysis project. *Bulletin of American Meteorological Society*, **77**, pp. 437–471.

Kaufman, Y.J., Taure, D., Remer, L.A., Vermote, E.F., Chu, A. and Holben, B.N., 1997, Operational remote sensing of tropospheric aerosol over land from EOS moderate resolution imaging spectroradiometer. *Journal of Geophysical Research*, **102**, pp. 17051–17067.

Korhonen, H., Carslaw, K.S., Forster, P.M., Mikkonen, S., Gordon, N.D. and Kokkola, H., 2010, Aerosols climate feedback due to decadal increases in southern hemisphere wind speeds. *Geophysical Research Letters*, **37**, L02805, doi:10.1029/2009GL041320.

Leon, J.F. and Legrand, M., 2003, Mineral dust sources in the surroundings of the north Indian Ocean. *Geophysical Research Letters*, **30**, pp. 1309–1315.

Levelt, P.F., Hilsenrath, E., Leppelmeier, G.W., Van Den Ooord, G.H.J., Bhartia, P.K., Taminnen, J., De Haan, J.F. and Veefkind, J.P., 2006, Science objectives of the ozone monitoring instrument. *IEEE Transactions on Geoscience and Remote Sensing*, **44**, pp. 1093–1101.

Levy, R.C., Remer, L.A., Kleidman, R.G., Mattoo, S., Ichoku, C., Kahn, R. and Eck, T.F., 2010, Global evaluation of collection 5 MODIS dark-target aerosol products over land. *Atmospheric Chemistry and Physics*, **10**, 10399–10420.

Pilnis, C., Pandis, S.N. and Seinfeld, J.H., 1995, Sensitivity of direct climate forcing by atmospheric aerosols to aerosol size and composition. *Journal of Geophysical Research*, **100**, pp. 739–754.

Rahul, P.R.C., Salvekar, P.S. and Devara, P.C.S., 2008, Aerosol optical depth variability over Arabian Sea during drought and normal years of Indian monsoon. *Geophysical Research Letters*, **35**, L22812, doi:10.1029/2008GL035573.

Rajeev, K., Ramanathan, V. and Meywerk, J., 2000, Regional aerosol distribution and its long-range transport over the Indian Ocean. *Journal of Geophysical Research*, **105**, pp. 2029–2043.

Remer, L.A., Kledman, R.G., Levy, R.C., Kaufman, Y.J., Tanre, D., Matto, S., Martins, J.V., Ichoku, C., Koren, I., Yu, H. and Holben, B.N., 2008, Global aerosol climatology from the MODIS satellite sensors. *Journal of Geophysical Research*, **113**, D14S07, doi:10.1029/2007JD009661.

Satheesh, S.K., 2002, Aerosol radiative forcing over tropical Indian Ocean: modulation by sea-surface winds. *Current Science*, **82**, pp. 310–316.

Satheesh, S.K. and Moorthy, K.K., 2005, Radiative effects of natural aerosols: a review. *Atmospheric Environment*, **39**, pp. 2089–2110.

Satheesh, S.K. and Srinivasan, J., 2002, Enhanced aerosol loading over Arabian Sea during pre-monsoon season: natural or anthropogenic. *Geophysical Research Letters*, **29**, 1874, doi:10.1029/2002GL015687.

Susan, K.G. and Prabha, R.N., 2008, Aerosol mass loading over the marine environment of Arabian Sea during ICARB: sea-salt and non-sea-salt components. *Journal of Earth System Science*, **117**, pp. 333–344.

Vinoj, V. and Satheesh, S.K., 2003, Measurements of aerosol optical depth over Arabian Sea during summer monsoon season. *Geophysical Research Letters*, **30**, 1263, doi:10.1029/2002GL016664.